The Role of Cis-Acting Genetic Regulation on Human Zinc Transporter SLC39A8

Barb Bohacova

Audrey Papp, Beth Besecker, Ilya Ioschikhes, Wolfgang Sadee, and Daren Knoell

ABSTRACT

We previously reported that zinc deficiency predisposes the lung epithelium to apoptosis during conditions of inflammatory stress.[1] Human zinc transporters comprise a family of 24 proteins and have a primary role in zinc homeostasis. All 24 transporters were examined in human epithelial cells and shown to have consistent levels of expression from donor to donor.[2] We have previously observed that primary cultures of human upper airway epithelia obtained from multiple human donors exhibit a marked induction in SLC39A8 gene expression when exposed to the inflammatory cytokine tumor necrosis factor alpha (TNFα). In sharp contrast, expression of all other zinc transporters remains largely unchanged. Therefore, we contend that genetic variability in SLC39A8 may confer changes in zinc regulation leading to differences in inter-individual variation in response to inflammatory stress.

The NIH SNP database was used to identify two candidate SNPs of high frequency (<40%) in the 3' UTR region (rs.9331& rs.9705) and one nonsynonymous SNP in the exon region (rs.13107325) of SLC39A8. Using PCR amplification and restriction enzyme digestion, 89 human small bowel samples were genotyped for each SNP. A SNaPshot assay was used to identify cis-acting genetic variability, in the form of allelic expression imbalance (AEI), in all heterozygous samples for each SNP. The promoter region was studied *in silico* to identify SNPs that harbored within transcription factor binding sites (TFBs). SnaPshot analysis revealed allelic imbalance in 1 sample out of a total of 28 heterozygous samples (obtained from 89 original donors).

The overall frequency of cis-acting dysfunction in SLC39A8 gene

expression appears to be minimal, but conditions in cytokine induced cells as well as lung epithelial cells remains to be studied. The promoter region shows that candidate SNPs do exist within putative TFBs and will be evaluated in future studies.

INTRODUCTION

Pulmonary diseases such as asthma and adult respiratory distress syndrome (ARDS) are a substantial burden to patients and society. Despite recent advances in medical research, the pathogenesis of these disorders are still not fully understood. Therefore, further investigation in this area is warranted. A common phenomenon observed in individuals with acute lung injury is degradation of the lung epithelium, a critical cellular barrier that protects the lung from the outer environment and maintains the ability on the host to ventilate.[1] In an attempt to understand the cause of lung epithelial cell damage, experiments have recently been conducted in the laboratory of my faculty supervisor demonstrating that zinc depletion induces cell apoptosis, also known as programmed cell death, and breakdown of the epithelial barrier.[1] The study showed that lung epithelial cells require zinc in order to tolerate an inflammatory environment and perhaps more importantly, that zinc supplementation protects cells from experiencing an untimely death. Therefore it is evident that zinc plays an important role in helping epithelial cells avoid apoptosis when in a hostile environment. In studies that I initiated, we observed that primary human lung epithelial cells possess an intricate system composed of 24 different zinc transporters that we presume allow these cells to maintain a critical intracellular zinc concentration. In general there are two major categories of zinc transporters. There are 14 zinc importers (SLC39A1 thru SLC39A14) reside on the cell membrane and transport zinc from the outside environment into the cell, and 10

zinc exporters (SLC30A1 thru SLC30A10) that function to export excess zinc out of the cell. In order to gain a better understanding of the role that these zinc transporters have within the epithelium, we developed a method to rapidly evaluate and quantify message RNA (mRNA) levels of all 24 zinc transporters in tandem. Primary lung epithelial cell cultures obtained from ten different human lung donors were screened for all 24 transporters in order to determine the amounts of mRNA expression of each gene. The results showed that the majority of all transporters were expressed across all donors to varying degree (Figure 1). We then conducted a similar experiment to measure the relative amounts of mRNA present when the cells were exposed to inflammatory cytokines, known to be upregulated in the lung environment during ARDS, as well as zinc deprivation. When cells were treated with Tumor Necrosis Factor-alpha (TNFα), a pro-inflammatory cytokine that is expressed early in patients with acute lung injury and ARDS, we observed that the zinc importer SLC39A8 was consistently and substantially up-regulated while the mRNA levels of most other transporters remained relatively unchanged (Figure 2). With this information it became apparent that SLC39A8 may play a critical role in regulating intracellular zinc during inflammatory stress and that an inspection of this gene was warranted to determine if genetic variability, that is single nucleotide polymorphisms (SNPs), in either the promotion region, protein coding region, or 3' untranslated region, could account for alteration in zinc homeostasis and disease susceptibility during inflammatory stress and the development of ARDS (Figure 3). A library of small bowel samples was used for further studies due to a limited amount of lung

tissue samples. The small bowel tissue contained the epithelium layer and was deemed readily suitable for our studies.

METHODS AND MATERIALS

Genetic Material Sources. For both the genotyping analysis and the allelic expression imbalance (AEI) assay, DNA and mRNA (in the form of cDNA) were obtained from a library of 89 small intestine samples from human donors. Isolation of DNA and mRNA was done using standard isolation procedures. For validation of the GC clamp assay a library of Coriell Cell Line cells were used. Coriell Cell's have been genetically mapped by the HapMap project. They were used to validate primer function because their genetic composition was known and readily available, as were the DNA samples from these cells.

Primer Design. Primer Express Software was used to design all primers. Guideline parameters for primer pairs were: i) amplification length of 50-150 bases ii) a melting point temperature of 58-60°C. iii) GC percent between 20-80% iv) primer length of 12-30 bases. For GC primers, two forward primers were designed to be allele specific. Each forward primer extends up to and including the SNP. The 3rd base from the 5' end of the primer was purposefully mismatched to the DNA sequence so as to ensure each primer's allele specific amplification. A 12 base long sequence of alternating G and C base pair was attached to only one forward primer. Forward primers were designed to minimize possible hairpin structures within each primer as well as dimer formation between the forward or reverse primers. A common reverse primer was designed to amplify with both forward primers.

A separate pair of forward and reverse primers were designed for the AEI

assay for SNPs rs.9331 and rs.13107325. Using optimum parameters, the primers were designed to amplify a 50-150 bases long region around the SNP. Also primer extension (PE) primers were designed for each SNP. Each PE primer was a forward primer that ran up to 1 base prior to the SNP of interest. The optimum melting temperature for the PE primer was set between 50-55°C.

Site directed mutagenesis (SDM) primers were designed to introduce a Cytosine instead of an Adenosine, three bases downstream from the SNP site of rs. 9705. The reverse primer introduced the mutagenesis site, extending up to a base pair before the SNP site. The forward primer was used just to amplify the sequence surrounding the SNP. All primers were used at a concentration of 10 μM in ddH_2O.

Genotyping. Initially GC clamp assays were designed for all three candidate SNPs. Three different types of genotype samples were chosen (homozygous A, heterozygous, & homozygous G and homozygous T, heterozygous & homozygous C, respectively), for rs.9331 and rs.9705. For rs.13107325 a random assortment of three individual samples were chosen. Each genotype was then amplified with the SNP primer, the wild type (WT) primer as well as both at the same time. Amplification was done using Real Time-Polymerase Chain Reaction (RT-PCR). Each reaction contained 10 μL of SYBR Green master mix, 8.8 μL of ddH_2O, 0.6 μL of Forward primer (the SNP, WT or both), 0.6 μL of reverse primer, and 1.0 μL of DNA. The sample wells were incubated at 50°C for 2 minutes, then at 95°C for 10 minutes, followed by 40 cycles of 95°C for 15

seconds, 60°C for 1 minute. A dissociation curve was also ran. To determine if product amplified before a cycle threshold of 30 cycles, as well as exhibiting correct dissociation behavior by evaluating melting curve differences based on amplification with a GC- or non-GC allele specific primer.

For rs.9705, the GC clamp assay proved to be insufficient for genotyping so the samples were amplified with SDM primers to amplify the SNP region sequence. Amplification was done using RT-PCR. Each reaction contained 10 µL of SYBR Green master mix, 8.8 µL of ddH_2O, 0.6 µL of forward primer, 0.6µL of reverse SDM primer, and 1.0 µL of DNA. To each sample was added 1.0µL of BstZ17 I restriction enzyme and 1.0 µL of NEBuffer3. Samples were incubated at 37°C overnight. Melting dissociation curves were run on all samples to observe differences in cut and un-cut product melting points. PCR products were then run on an agarose gel. Into each well was loaded 10 µL of PCR product (digested with enzyme) mixed with 2 µL of Orange tracking dye. One of the wells contained 12 µL of DNA ladder for sizing purposes. The gel was run at 80V for approximately 30 minutes. The results were viewed in a chamber with ultraviolet light.

Samples were then amplified in the same manner using a fluorescently labeled forward primer. PCR and digestion was conducted as previously described. The digested product was analyzed by capillary electrophoresis, using an ABI3730 instrument with a GeneScan 500 ROX standard in triplet repeats. This allowed us to determine peak size which correlated directly with base pair length, and genotype.

PCR Amplification. Heterozygous samples were amplified by standard PCR. Each sample well contained 7.5 µL of 2X Ready mix, 0.3 µL of forward primer, 0.3 µL of reverse primer, 5.9 µL of ddH_2O, and 1.0 µL of template (DNA or cDNA). The samples were denatured at 95°C for 2 minutes followed by 30 cycles of 95°C for 15 seconds, 60°C for 1 minute, and 72°C for 1 minute. To purify the products, exonuclease I (Exo I) was used to degrade residual single stranded primers. Bacterial Alkaline phosphatase (BAP) was used to prevent fragments from self-ligating. 1 µL of BAP, 0.1 µL of ExoI, and 1.4 µL of 10X buffer with Zinc was added to each reaction well. The samples were incubated at 37°C overnight and then incubated at 80°C for 15 minutes to inactivate the enzyme.

Primer Extension Optimization . Optimization of SNaPshot buffer and the PE primer was done using amplified samples 1 and 2. A total of 4 different combinations were used with both samples. Reactions wells were as follows. Combination 1: 2.5 µL of SNaPshot buffer, 0.5 µL of PE primer, 1.5 µL of PCR product, and 0.5 µL of ddH_2O. Combination 2: 2.5 µL of SNaPshot buffer, 0.25 µL of PE primer, 1.5 µL of PCR product, and 0.75 µL of ddH_2O. Combination 3: 1.25 µL of SNaPshot buffer, 0.5 µL of PE primer, 1.5 µLof PCR product, and 1.75 µL ddH_2O. Combination 4: 1.25 µLof SNaPshot buffer, 0.25 µL of PE primer, 1.5 µL of PCR product, and 2 µL of ddH_2O. Each reaction well was denatured at 95C for 2 minutes, followed by 25 cycles of 95°C for 10 seconds then 55°C for 5 seconds. 1 µL of Calf Intestinal Phosphatase (CIP) was added to each well, to

degrade any unincorporated fluorescently marked dideoxynucleotides (ddNTPs) and PE primers. The samples were incubated at 37°C overnight and then incubated at 80°C for 15 minutes to inactivate the enzyme.

SNaPshot. Products from the PE optimization were run through a capillary electrophoresis instrument, ABI 3730, using LIZ120 standard. Ratios of peak areas were analyzed using the GeneMapper v3.70 program (ABI). Analysis showed that Combination 3 provided optimal results therefore all further AEI was done using those parameters.

Promoter Analysis: The SLC39A8 promoter sequence was retrieved using the UCSC genome browser (http://genome.ucsc.edu) in collaboration with Dr. Ilya Ioshkes. The genomic sequence and 10kb upstream from the gene start site were analyzed. The putative transcription factor binding sites (TFBS) were mapped using MatchTM Professional software developed by Biobase International GmbH "MATCHTM (A tool for searching transcription factor binding sites in DNA sequences" **Nucleic Acids Res. 31, 3576-3579.**) The search was performed with high-quality matrices and with cutoff parameters minimizing false negative predictions.

All TFBS were matched up to known SNPs in the UCSC database. SNPs existing at the chromosomal positions of the TFBS were noted by position, name (reference #) as well as heterozygosity when possible.

RESULTS

Our initial work of measuring mRNA levels in human donors showed that relative amounts of mRNA were very consistent donor to donor (Figure 1). This shows that the regulation of these transporters is very tight and it is most likely inflammatory conditions which incite differences between patients. Due to the validation of the primers' capacities to amplify the sequences we were able to develop a semi-quantitative method of measuring relative mRNA levels that could be applied to both baseline and inflammatory conditions. Thus a consistent 9 fold increase in SLC39A8 mRNA levels during TNF-α induction is indicative of the importance of this gene during stress (Figure 2).

The first attempt using the GC clamp assay was not successful for any of the three SNPs. Not all samples were amplified to a sufficient amount (<30 cycle threshold) and dissociation curves did not show a clear distinction between genotypes. As a result, GC primers (Figure 4 a) were redesigned to improve amplification in the presence of the allele specific primers. The new primers were tested again with the Coriell Cell Line samples. Amplification and dissociation of the amplified product met criteria so we proceeded with genotyping of the small bowel samples (Figure 4 c).

SNP rs.13107325 is not in the HapMap project so samples of known genotype were not readily available to sufficiently test the efficiency of the GC clamp assay. However, due to the low heterozygosity (4.2%) of this SNP, it was decided to use a primer that amplifies the SNP allele only, and therefore eliminating complications of amplification with two primers in the same sample.

Amplification with the SNP primer resulted in the identification of 7 samples (Figure 4 b) that were either heterozygous or homozygous for the SNP.

All 7 samples were then amplified using fluorescent ddNTPs along with PE primers. The SNaPshot assay revealed that 1 sample (patient #19) was in fact homozygous T while the rest of the 6 samples were heterozygous. The average ratio of C to T allele levels was 0.2917 to 0.7083. Also the average standard deviation of mRNA levels from DNA levels was only 0.855% (Appendix C). The results show that none of the heterozygotes exhibited AEI (Figure 6 c).

The standard GC clamp assay was used to genotype SNP rs.9331. Of the 89 samples genotyped, 27 were heterozygous, 51 were homozygous A, 6 were homozygous G, and 5 were not able to be analyzed (Figure 6 a). The genotype was based on dissociation curves of the amplified products. Of all 27 heterozygous samples, 24 were available for SNaPshot analysis. The results of the SNaPshot assay revealed that the DNA of all samples was consistently comprised of an average ratio of 0.4214 to 0.5785 G to A allele levels. DNA levels from sample to sample were consistent, with an average standard deviation of 2.38%. Deviation of mRNA levels compared to DNA in the same patient was found to be even less with an average deviation, for all samples, of 1.88% (Appendix A). This shows that the DNA is consistent from sample to sample as would be expected, since a 1:1 ratio ought to be observed, one from each allele. A ratio of 0.4214 to 0.5785 (of guanine to adenosine levels) was observed because the fluorescently labeled Adenosine fluoresces more strongly than the Guanine.

Of the 24 samples analyzed, 1 sample (sample #48) showed a consistent decrease in SNP mRNA levels compared to the DNA levels (Figure 7). The DNA ratio of G to A, (or SNP to WT) levels was 0.4374 to 0.5626. The mRNA ratio of G to A levels were on average 0.2972 to 0.7028. This is a 46% decrease in relative amounts of the G allele (the SNP allele) mRNA compared to DNA (Appendix A).

The GC clamp method could not be used to genotype SNP rs.9705. So the samples were genotyped using the restriction enzyme BstZ17I after introducing a mutagenesis site that allowed the samples to be distinguished by alleles. Samples were first amplified with non-fluorescent primers. DNA was then amplified using RT-PCR. The dissociation curves showed no distinguishable peaks between digested and undigested samples. When run on an agarose gel, band resolution was poor and we could no identify cut and uncut PCR products. Also, the smallest marker on the ladder was 100bp so smaller bands of 65 and 40bp were hard to distinguish.

To overcome this, samples were again amplified with a fluorescently marked forward primer. After digestion and separation with capillary electrophoresis, genotyping was possible. Samples with the C allele exhibited a peak at 65bp, while samples with a T allele exhibited a peak at 40bp. Heterozygotes (with both a C and T allele) exhibited peaks at both lengths (Figure 5). Of the 89 samples analyzed, 48 were homozygous C (or WT), 10 were homozygous T (or SNP), while 19 samples were heterozygous, and 12 samples were not able to be analyzed (Figure 6 b).

The SNaPshot assay was then conducted with standard procedure. An extra calf intestine phosphatase digestion was conducted to remove extraneous fragments that hindered data analysis. Upon the second run through capillary electrophoresis instrument, samples were analyzed and showed to be more variant than for either of the other two SNPs. The average C to T ratio was 0.3980 to 0.6020, while the average standard deviation of DNA was a high at 7.71%. Variation of mRNA to DNA levels in the same patient was much lower, with an average standard deviation of 4.92% (Appendix B). Of all samples tested, no consistent deviation was observed in mRNA with respect to the patients DNA.

The variation in the results for rs.9705 is most likely due inherent errors in the extension process. Variation in the DNA levels is mostly due to irregular amplification and extension with the PE primers because all DNA samples had one SNP and one WT allele. Because the DNA acts as an internal standard, what we are looking for is a consistency in the variation of the levels of mRNA compared to DNA, which was not found in these samples.

Computer analysis yielded 5 different TFBS present in the promoter region of SLC39A8. Of those 5, 3 (AP-1, MEF-2 and NFκB) were found to contain SNPs present in their binding domains. The SNPs were of a variety of heterozygosities, some of which were exhibit a high frequency and thus a great deal of potential for further study (Figure 8).The SNPs found in these putative sites could impact the initiation of gene transcription, and therefore allelic expression.

CONCLUSION

We were the first to observe that the human zinc transporter SLC39A8 is substantially upregulated by cytokines, in comparison to all other zinc transporters, in human lung epithelia. Based on this observation we contend that SLC39A8 is critical in regulating zinc homeostasis and cell function during inflammatory stress. Further evaluation of the SLC39A8 gene revealed multiple frequently occurring SNPs thereby suggesting that genetic regulation may influence cell function. Based on this we wanted to determine if frequently occurring SNPs could confer changes in cell function via cis-acting genetic regulation. As a first step, three candidate SNPs were identified in the SLC39A8 gene and investigated for allelic imbalance. Our analysis was conducted in a collection of human small intestine samples since a large collection of human lung epithelia was not available at the time of this study.

Genotype analysis of all samples was in range with the reported heterozygosity of each SNP studied. For SNP rs.9331 the experimental heterozygosity was 30% (24 out of 81 samples), while the reported value is 48.5%. For SNP rs.9705 the experimental heterozygosity was found to be 25.6% (20 out of 78 samples)while the reported value is 47.8%. Finally for SNP rs.13107325 we found the heterozygosity to be 5.7% (5 out of 88 samples) while the reported value is 4.6%.(www.genecards.com) We attribute the deviation in heterozygosity between observed and reported percentages to a relatively small sample size, as many more samples would be necessary in order to get a more accurate measure of heterozygosity.

Evaluation of allelic expression imbalance demonstrated no evidence of imbalance in two out of the three SNPs studied (rs.9705 and rs.13107325). This observation suggests that these SNPs confer no direct contribution to cis-acting genetic regulation and likely do not directly impact mRNA expression of SLC39A8. As for SNP rs.9331, one sample out of 24 heterozygous samples demonstrated allelic imbalance. The amount of mRNA containing the variant allele was 46% lower than the normal allele. Although this doesn't prove that rs.9331 directly impacts mRNA levels, this observation indicates that cis-acting gene regulation does exist in SLC39A8. The frequency of allelic imbalance was 3.6% (1 out of 28 samples) in a repository of human small bowel samples. Further study would be necessary to link allelic imbalance to rs.9331 as well as other SNPs within the gene and the promoter region. Also conducting an AEI assay with human lung epithelial cells exposed to inflamatory cytokines, would be necessary to observe any differences in mRNA level expression.

Evaluation of transcription factor binding sites in the promoter region revealed several SNPs in potential putative TNFα-inducible transcription initiation start sites. This suggests that other candidate SNPs that influence SLC39A8 gene expression during inflammatory stress may exist. Promoter analysis was conducted *in silico* and will require further evaluation with methods utilized in this study.

We have observed that zinc is a potent cytoprotectant in human lung epithelia. In particular, zinc depletion significantly increases lung epithelial cell death following exposure to inflammatory cytokines whereas in sharp contrast,

intracellular zinc repletion at the onset of inflammation prevents cell death. Our interpretation of these findings is that zinc uptake into the lung epithelium via zinc transporters is an essential innate host protective response that prevents cell death. Our results also suggest that abnormal zinc homeostasis, either due to dietary insufficiency or polymorphic variation in proteins that regulate zinc homeostasis may increase host susceptibility to cell damage and tissue dysfunction.

Our findings demonstrate that genetic variability in SLC39A8 may be a cause for lung tissue dysfunction. Although the data was taken from human bowel samples, it identifies that cis-acting genetic imbalance exists in humans. Based on this, we hypothesize that “state-dependant” conditions such as inflammatory stress, may amplify the impact of SNPs located in the SLC39A8 gene and play an important role in regulating zinc homeostasis during inflammation and the host protective response. Further evaluation using human lung samples is warranted.

REFERENCES

1. Shenying Bao and Daren L Knoell. Zinc Modulates Airway Epithelium Susceptibility to Death Receptor-Mediated Apoptosis. *Am J Physiol Lung Cell Mol Physiol* (November 11, 2005). doi:10.1152/ajplung.00341.2005

2. Knoell DL, Sadee W, Papp A, Johnson A, Bohacova B, Besecker B.Modulation of Zinc Transporter RNA Expression by TNFa in Human Lung Epithelia. Abstract submitted to ATS.The Ohio State University Davis Heart and Lung Research Institute. Columbus, OH

ACKNOWLEDGEMENTS

Financial Support: NIH HL04462 (DLK) and GM61390 (WS). I also thank the Honors College for a research scholarship.

Support of this research by the Department of Chemistry and Professor T. V. RajanBabu is gratefully acknowledged.

FIGURE LEGENDS

Figure 1. Expression of all 24 Human Zinc Transporters. A total of 8 donors were profiled for expression levels of zinc transporters in lung epithelium tissue.

Figure 2. Expression of the Human Zinc Transporter SLC39A8 is Induced by Tumor Necrosis Factor alpha (TNFα). SLC39A8 mRNA was significantly up-regulated in comparison to all other zinc transporters following 24 hour exposure to TNFα in primary cultures of human lung epithelial.

Figure 3. A map of the human zinc transporter SLC39A8. Two high frequency SNPs in the 3'UTR region and one non-synonymous SNP in the coding region of SLC39A8 were identified as candidate SNPs for further evaluation of cis-acting gene regulation.

Figure 4. Genotype analysis using a GC clamp assay and RT-PCR. This is an example of an Allele Specific Primer. The primer extends only the G allele because the 3rd letter is mismatched. (Figure A) Positive samples amplified before PCR cycle #30 (blue line) while negative samples did not (red line). (Figure B) Homozygous G samples had a peak at 72˚C, homozygous A samples had a peak at 77˚C (due to GC tail on primer) while heterozygous samples had peaks at both temperatures. (Figure C)

Figure 5. Genotyping using a restriction enzyme and capillary electrophoresis. After treatment of PCR product with the restriction enzyme BSTZ17I, homozygous A samples had a peak at 40 bases (length of cut amplification product), while homozygous G samples had a peak at 65 bases (uncut product). Heterozygous samples had peaks at 40 and 65 bases.

Figure 6. Results of all genotype analyses for all three SNPs. Algorhythm for results obtained for SNP rs.9331.(Figure A) Algorhythm for results obtained for SNP rs.9705.(Figure B) Algorhythm for results obtained for SNP rs.13107325. (Figure C)

Figure 7. Example of AEI Analysis in Heterozygous Samples. *Patient #21:* Ratio of G allele expression to A allele expression is consistent in mRNA (bottom two graphs) with DNA (top graph). *Patient # 48*: Ratio of G to A alleles is higher in DNA and consistently lower in mRNA levels. Patient #48 demonstrates allelic imbalance in mRNA expression.

Figure 8. SNPs Occur in TNFα-Inducible Transcription Factor Binding Sites. Results of promoter region analysis are presented. Five transcription factor binding (TFB) sites were identified. SNPs were identified in AP-1, MEF-2, and NFκB regions.

Figure 1

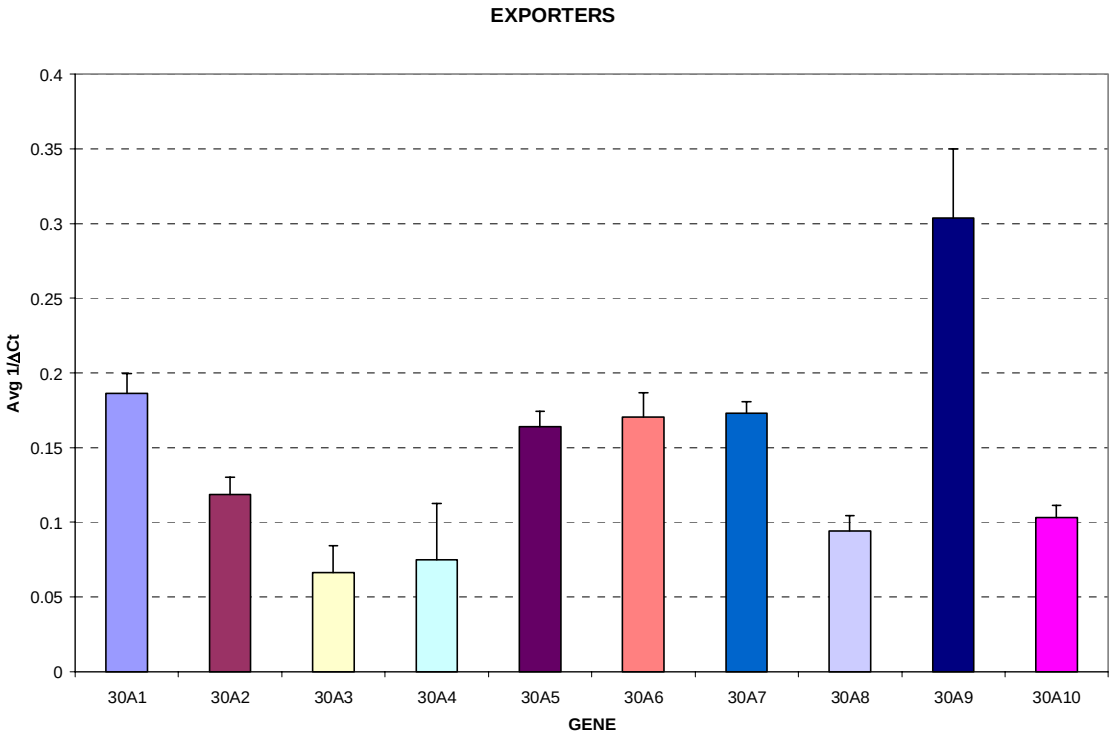
EXPORTERS
Avg 1/ΔCt
0.4
0.35
0.3
0.25
0.2
0.15
0.1
0.05
0
30A1
30A2
30A3
30A4
30A5
30A6
30A7
30A8
30A9
30A10
GENE

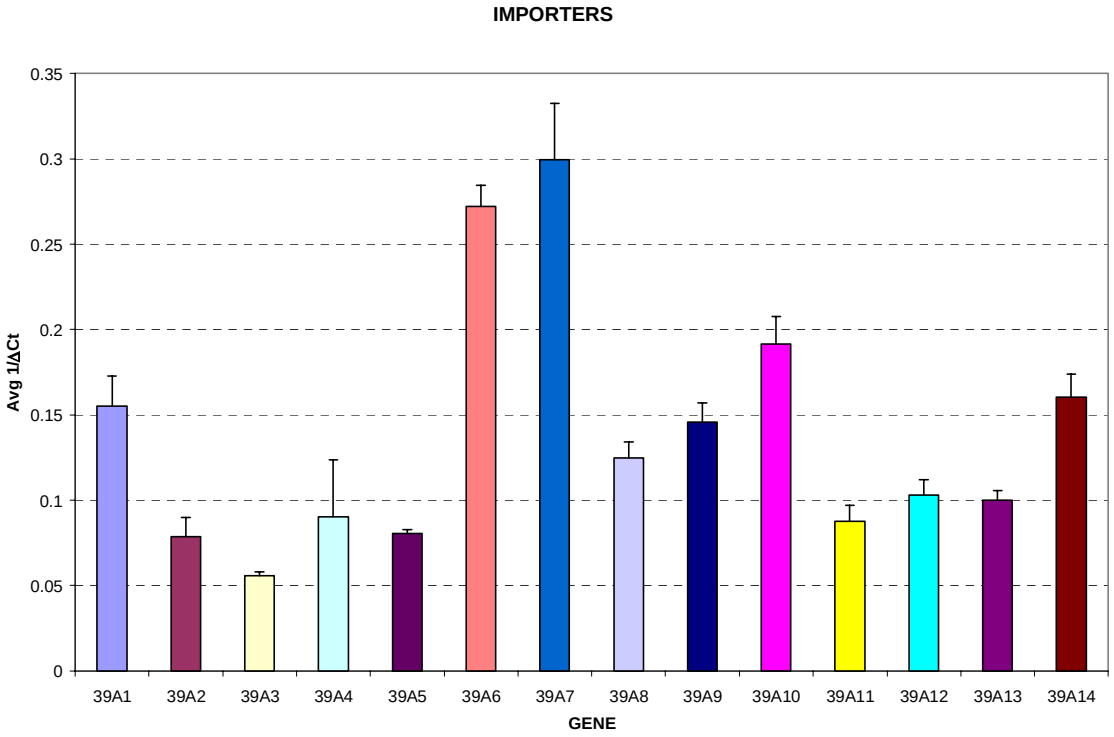
IMPORTERS
Avg 1/ΔCt
0.35
0.3
0.25
0.2
0.15
0.1
0.05
0
39A1
39A2
39A3
39A4
39A5
39A6
39A7
39A8
39A9
39A10
39A11
39A12
39A13
39A14
GENE

Figure 2

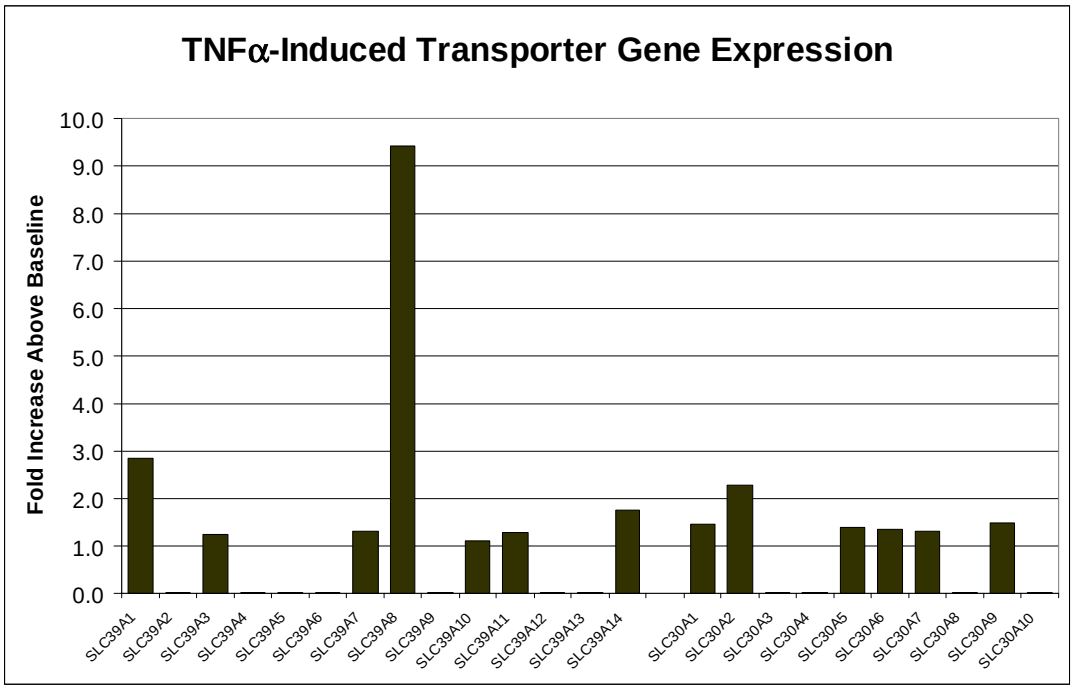
TNFα-Induced Transporter Gene Expression
Fold Increase Above Baseline
10.0
9.0
8.0
7.0
6.0
5.0
4.0
3.0
2.0
1.0
0.0
SLC39A1
SLC39A2
SLC39A3
SLC39A4
SLC39A5
SLC39A6
SLC39A7
SLC39A8
SLC39A9
SLC39A10
SLC39A11
SLC39A12
SLC39A13
SLC39A14
SLC30A1
SLC30A2
SLC30A3
SLC30A4
SLC30A5
SLC30A6
SLC30A7
SLC30A8
SLC30A9
SLC30A10

Figure 3

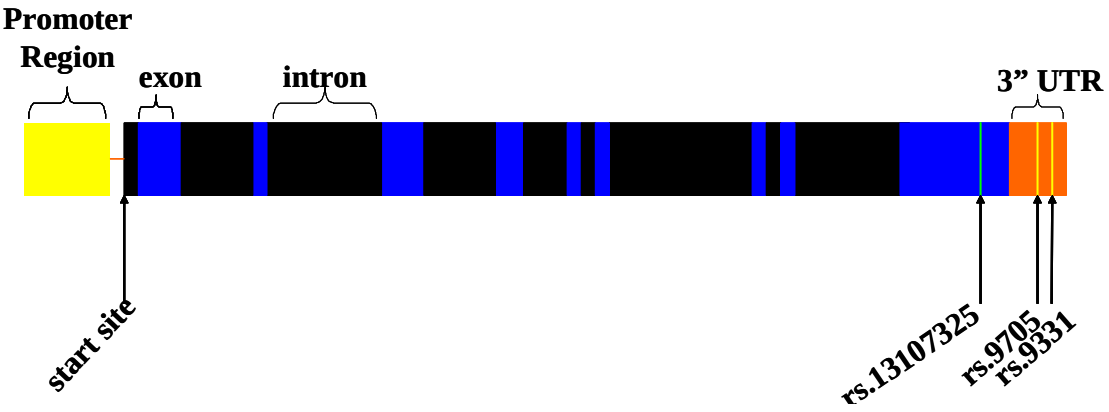
Promoter Region
exon
intron
3” UTR
start site
rs.13107325
rs.9705
rs.9331

Figure 4

A

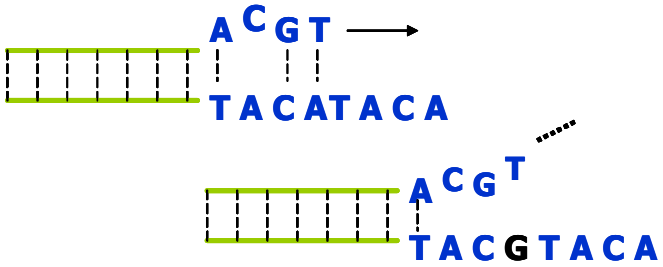
A C G T
T A C A T A C A
A C G T
T A C G T A C A

B

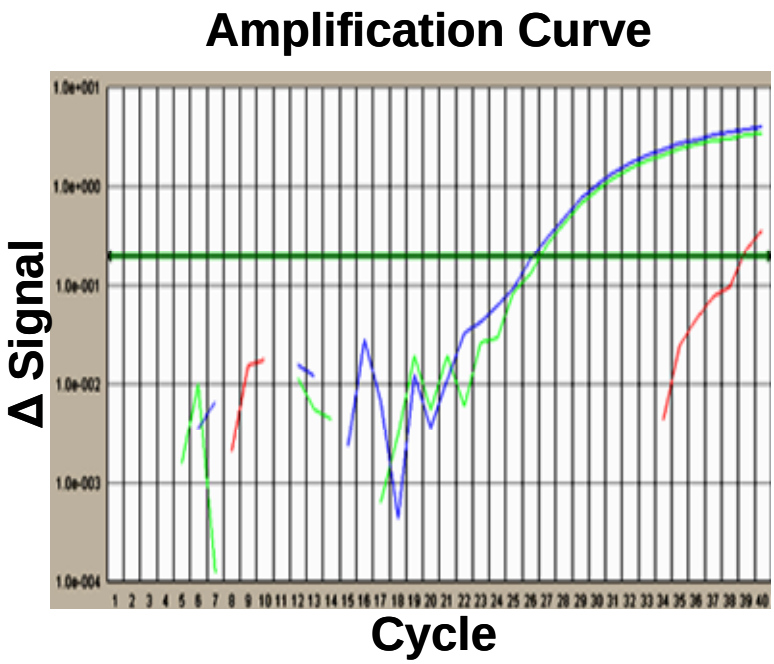
Amplification Curve
Δ Signal
Cycle

C

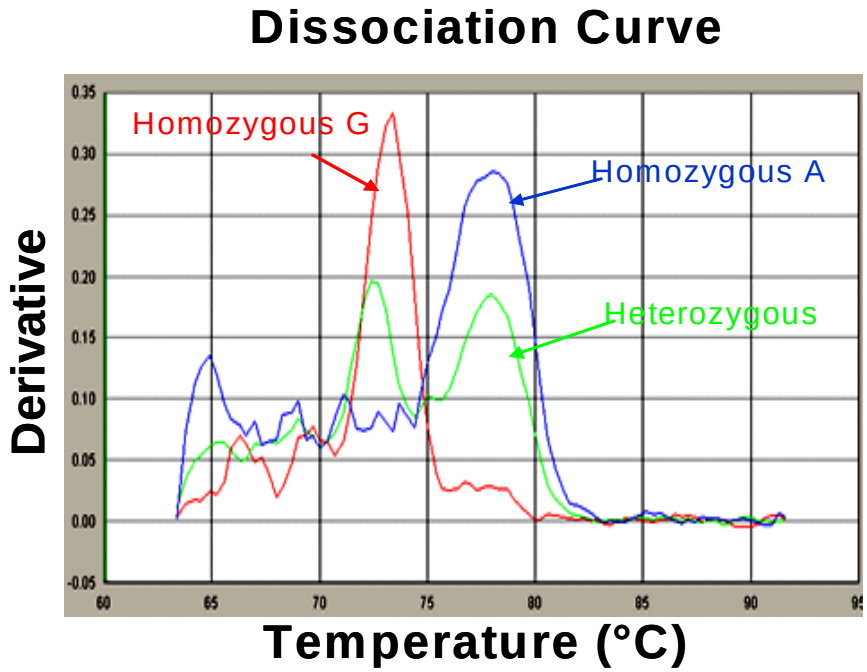
Dissociation Curve
Homozygous G
Homozygous A
Heterozygous
Derivative
Temperature (°C)

Figure 5

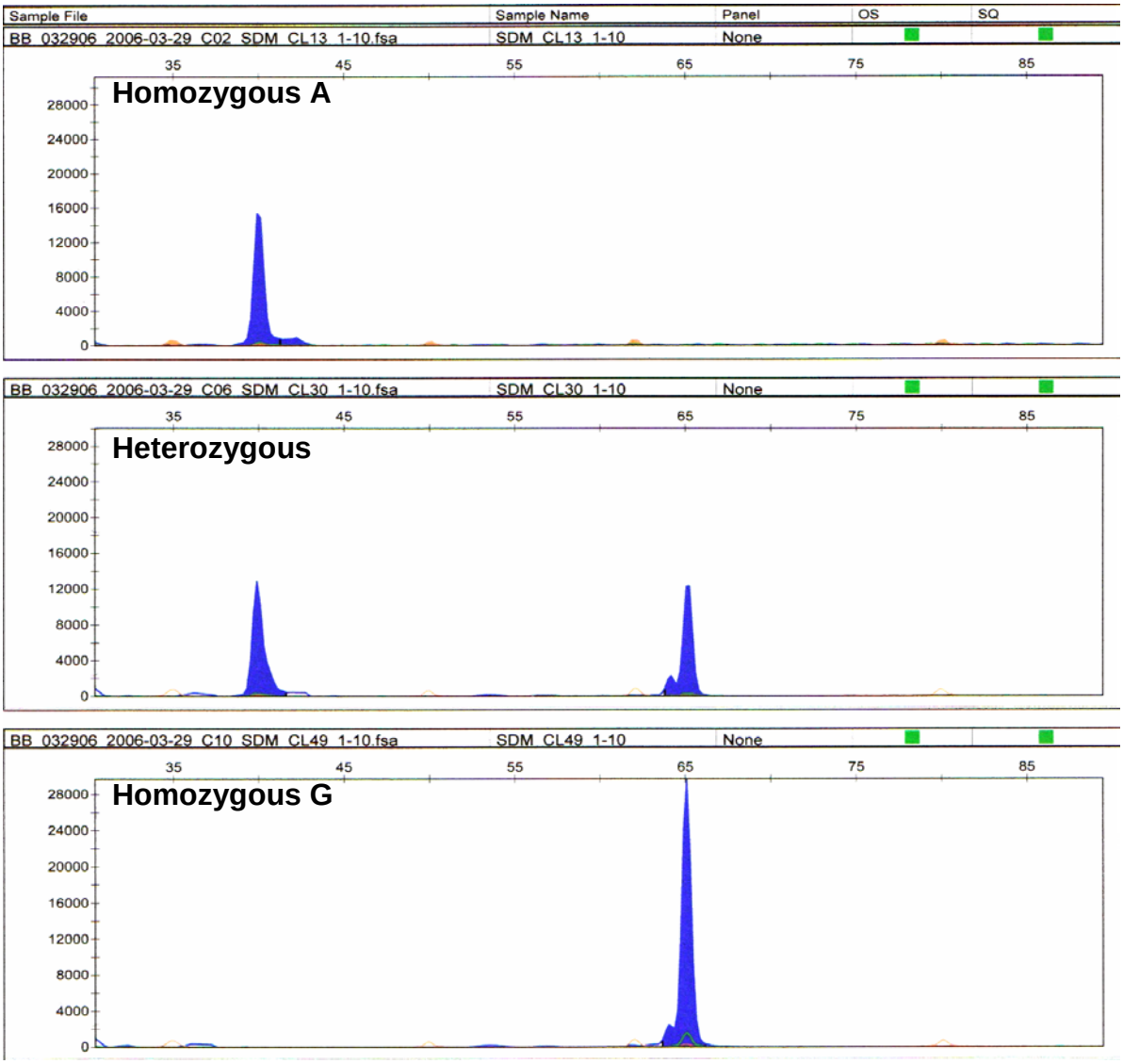
Sample File
Sample Name
Panel
OS
SQ
BB_032906_2006-03-29_C02_SDM_CL13_1-10.fsa
SDM_CL13_1-10
None
Homozygous A
BB_032906_2006-03-29_C06_SDM_CL30_1-10.fsa
SDM_CL30_1-10
None
Heterozygous
BB_032906_2006-03-29_C10_SDM_CL49_1-10.fsa
SDM_CL49_1-10
None
Homozygous G
35
45
55
65
75
85
28000
24000
20000
16000
12000
8000
4000
0

Figure 6

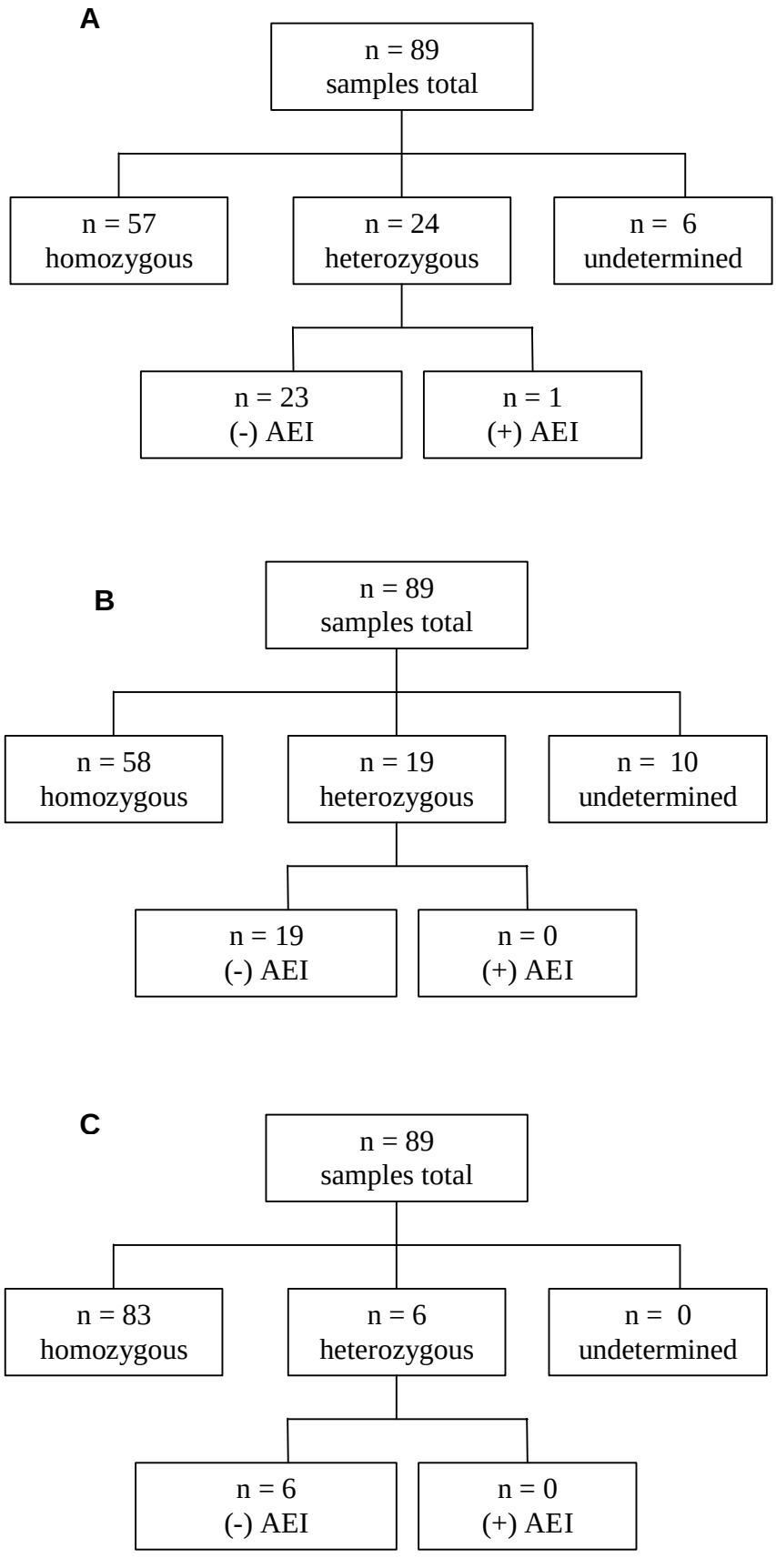
A
n = 89
samples total
n = 57
homozygous
n = 24
heterozygous
n = 6
undetermined
n = 23
(-) AEI
n = 1
(+) AEI
B
n = 89
samples total
n = 58
homozygous
n = 19
heterozygous
n = 10
undetermined
n = 19
(-) AEI
n = 0
(+) AEI
C
n = 89
samples total
n = 83
homozygous
n = 6
heterozygous
n = 0
undetermined
n = 6
(-) AEI
n = 0
(+) AEI

Figure 7

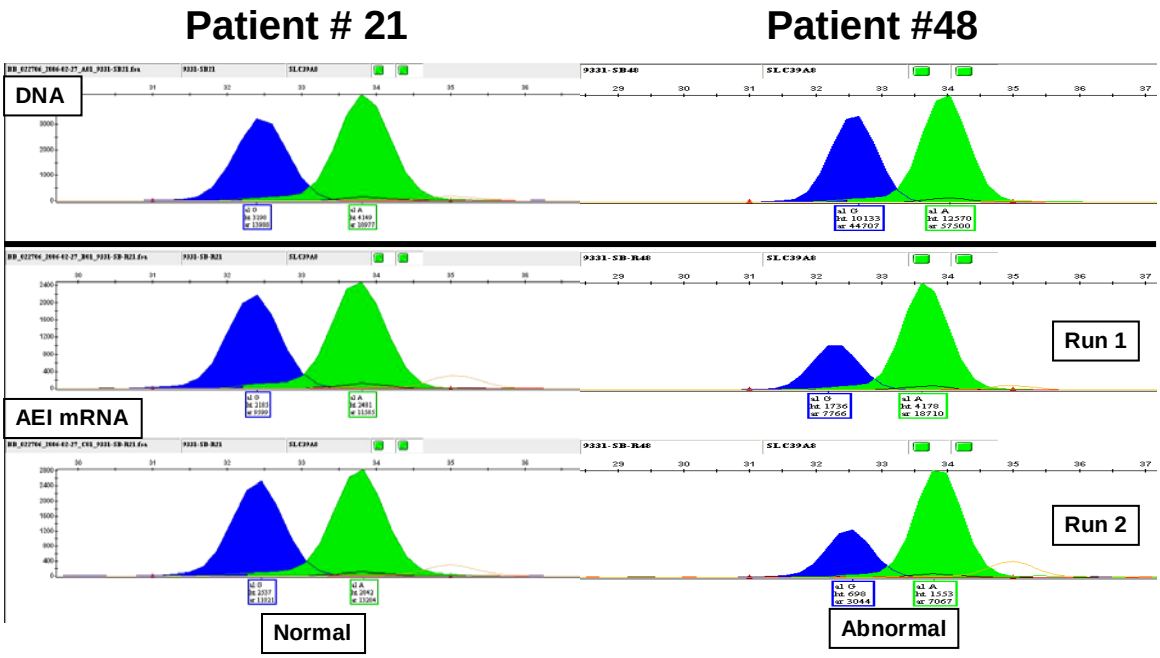
Patient # 21
Patient #48
DNA
AEI mRNA
Run 1
Run 2
Normal
Abnormal

Figure 8

TFB	SNP	Heterozygosity
AP-1	10642484	N/A
	10683672	N/A
	1381893	0.500 +/- 0.007
	6844796	N/A
	10461136	N/A
	11940755	N/A
	10222784	N/A
MEF-2	13152048	0.159+/-0.233
	6846162	N/A
	4699015	N/A
	11282386	N/A
	4557261	0.448+/-0.152
	7655997	N/A
	7681842	N/A
	7684449	N/A

TFB	SNP	Heterozygosity
NFkappaB	7695247	0.014+/-0.083
	4146610	N/A
	7655997	N/A
	10683672	N/A
	1350992	N/A
	17212693	0.106+/-0.205
	7664683	0.225+/-0.249
	7376560	N/A
POU	NONE	NONE
C/EBP	NONE	NONE

Appendix A – SNP rs. 9331

sample	#	%G	%A	std dev G	std dev A
DNA	21	0.424329	0.575671	0.01401939	0.01402273
RNA	21	0.453125	0.546875		
RNA	21	0.45493	0.545057		
DNA	25	0.436203	0.563797	0.01216472	0.01216472
RNA	25	0.411522	0.588478		
RNA	25	0.438321	0.561679		
DNA	33	0.447766	0.552234	0.00317134	0.00317134
RNA	33	0.440335	0.559665		
RNA	33	0.44209	0.55791		
DNA	41	0.419948	0.580052	0.01234717	0.01234756
RNA	41	0.450067	0.549933		
RNA	41	0.437389	0.562602		
DNA	47	0.439963	0.560037	0.04031809	0.04031809
RNA	47	0.346827	0.653173		
RNA	47	0.421842	0.578158		
DNA	48	0.437416	0.562584	0.06617857	0.06617857
RNA	48	0.293322	0.706678		
RNA	48	0.301058	0.698942		
DNA	51	0.419054	0.580946	0.01223915	0.01223915
RNA	51	0.420095	0.579905		
RNA	51	0.445522	0.554478		
DNA	54	0.41203	0.58797		
DNA	55	0.399138	0.600862	0.02081344	0.0209761
RNA	55	0.366285	0.633715		
RNA	55	0.348949	0.651501		
DNA	67	0.414721	0.585279	0.00014296	0.00014056
RNA	67	0.414689	0.585302		
RNA	67	0.415007	0.584993		
DNA	73	0.409121	0.590879	0.00802483	0.00802483
RNA	73	0.424283	0.575717		
RNA	73	0.427536	0.572464		
DNA	75	0.39251	0.607149	0.0057938	0.00587601
RNA	75	0.38021	0.61979		
RNA	75	0.392491	0.607509		
DNA	76	0.374549	0.625451	0.01915969	0.01915969
RNA	76	0.401011	0.598989		
RNA	76	0.421347	0.578653		
DNA	77	0.400906	0.599094	0.05424349	0.05424349
RNA	77	0.276367	0.723633		
RNA	77	0.378738	0.621262		
DNA	78	0.42308	0.57692	0.01801093	0.01775456
RNA	78	0.383571	0.615429		
RNA	78	0.386324	0.613676		
DNA	79	0.500971	0.499029	0.03090212	0.03090212
RNA	79	0.432314	0.567686		
RNA	79	0.43904	0.56096		
DNA	80	0.428618	0.571382	0.00749785	0.00749785

RNA	80	0.418358	0.581642		
RNA	80	0.43668	0.56332		
DNA	87	0.413745	0.586255	0.0189556	0.0189556
RNA	87	0.396021	0.603979		
RNA	87	0.442049	0.557951		
RNA	89	0.397547	0.602453	0.014017	0.014017
RNA	89	0.425581	0.574419		
DNA	81	0.443081	0.556919	0.02296052	0.02326726
RNA	81	0.482194	0.517806		
RNA	81	0.427638	0.573262		
DNA	2	0.4083	0.5917	0.01864824	0.01864824
RNA	2	0.422076	0.577924		
RNA	2	0.377471	0.622529		
DNA	8	0.41177	0.58823	0.01826237	0.0182906
RNA	8	0.375923	0.624077		
RNA	8	0.417021	0.582879		
DNA	12	0.423459	0.576541	0.0113015	0.0113015
RNA	12	0.400856	0.599144		
DNA	20	0.412379	0.587621	0.002391	0.002391
RNA	20	0.417851	0.582149		
RNA	20	0.416923	0.583077		
Average	**DNA**	**0.42143726**	**0.57854791**	**0.01876364**	**0.01877776**
Standard	**Deviation**	**0.02379722**	**0.02377929**		

Appendix B – SNP rs.9705

Sample	#	%C	%T	Std Dev
DNA	1	0.341727	0.658273	0.0628745
RNA	1	0.467476	0.532524	
DNA	12	0.403483	0.596517	0.02931156
RNA	12	0.378073	0.621927	
RNA	12	0.332623	0.667377	
DNA	20	0.299629	0.700371	0.01968402
RNA	20	0.347652	0.652348	
RNA	20	0.31991	0.68009	
DNA	21			
RNA	21	0.386423	0.613577	0.001368
RNA	21	0.389159	0.610841	
DNA	33	0.395055	0.604945	0.04037903
RNA	33	0.321838	0.678162	
RNA	33	0.300857	0.699143	
DNA	41	0.307163	0.692837	0.07849143
RNA	41	0.260258	0.739742	
RNA	41	0.445185	0.554815	
DNA	47	0.475519	0.524481	0.06928014
RNA	47	0.314149	0.685851	
RNA	47	0.440316	0.559684	
DNA	48	0.390201	0.609799	0.02235282
RNA	48	0.444597	0.555403	
RNA	48	0.422805	0.577195	
DNA	51	0.400482	0.599518	0.01711019
RNA	51	0.438168	0.561832	
RNA	51	0.435207	0.564793	
DNA	62	0.503333	0.496667	0.06034645
RNA	62	0.388907	0.611093	
RNA	62	0.365079	0.634921	
DNA	73	0.322624	0.677376	0.02753962
RNA	73	0.267385	0.732615	
RNA	73	0.328537	0.671463	
DNA	75	0.442297	0.557703	0.01297335
RNA	75	0.457743	0.542257	
RNA	75	0.474071	0.525929	
DNA	76	0.459205	0.540795	0.06838156
RNA	76	0.3267	0.6733	
RNA	76	0.304217	0.695783	
DNA	77	0.262422	0.737578	0.10142396
RNA	77	0.506547	0.493453	
RNA	77	0.344573	0.655427	
DNA	78	0.533295	0.466705	0.05170758
RNA	78	0.481808	0.518192	
RNA	78	0.407335	0.592665	
DNA	79	0.365365	0.634635	0.03052027
RNA	79	0.301362	0.698638	
RNA	79	0.299906	0.700094	

DNA	80	0.326452	0.673548	0.08265053
RNA	80	0.527097	0.472903	
RNA	80	0.403404	0.596596	
DNA	81	0.539395	0.460605	0.06257872
RNA	81	0.447623	0.552377	
RNA	81	0.38718	0.61282	
DNA	87	0.384303	0.615697	0.07650383
RNA	87	0.246632	0.753368	
RNA	87	0.425571	0.574429	
DNA	89	0.409816	0.590184	0.06812839
RNA	89	0.531892	0.468108	
RNA	89	0.372316	0.627684	
Average	**DNA**	**0.39798768**	**0.60201232**	**0.0491803**
Standard	**Deviation**	**0.07707983**	**0.07707983**	

Appendix C – SNP rs. 13107325

Sample	#	%C	%T	Std Dev
RNA	4	0.272375	0.727625	0.015332
RNA	4	0.303039	0.696961	
RNA	29	0.2978	0.7022	0.0048
RNA	29	0.3074	0.6926	
DNA	30	0.3016	0.6984	0.00835
RNA	30	0.2849	0.7151	
DNA	38	0.2973	0.7027	0.0015
RNA	38	0.3003	0.6997	
RNA	72	0.267	0.733	0.01585
RNA	72	0.2987	0.7013	
DNA	74	0.2763	0.7237	0.00545
RNA	74	0.2654	0.7346	
Average	**DNA**	**0.29173333**	**0.70826667**	**0.008547**
Standard	**Deviation**	**0.01353748**	**0.01353748**	